Large-Dynamic Frequency Response Measurement for Broadband Electro-Optic Phase Modulators

Yuqing Heng, Min Xue, *Member, IEEE*, Wei Chen, Shunli Han, Jiaqing Liu, and Shilong Pan, *Senior Member, IEEE*

***Abstract*— A novel method for characterizing the frequency responses of broadband electro-optic phase modulators (PMs) by employing stimulated Brillouin scattering (SBS) is proposed and experimentally demonstrated. In the proposed method, the SBS amplifies the +1st-order sideband and attenuates the −1st-order sideband of the phase-modulated signal from a PM under test. Thereby, the phase-modulated signal is converted into an optical single-sideband modulation signal. After square-law photodetection, the overall frequency responses are obtained. Removing the frequency responses of the SBS gain and the photodetector from the overall responses, the responses of the PM are thus achieved. Benefitting from the amplification of the SBS, the proposed method possesses a large dynamic range. Sub-Hz resolution and broadband measurement range are also achievable. A commercial broadband PM is experimentally characterized from 10 MHz to 50 GHz with a resolution of 5 MHz. According to the amplification of the SBS, the dynamic range is enhanced by 17.74 dB. The measurement result is verified by the conventional method utilizing optical spectrum analysis.**

***Index Terms*— Electrooptic modulation, phase modulation, microwave photonics, optical variables measurement, stimulated Brillouin scattering.**

I. Introduction

BROADBAND electro-optic phase modulators (PMs) are now fundamental electrical-to-optical conversion components in high-speed communications [1] and microwave photonics [2]–[4] due to the intrinsic advantages of high linearity, bias-free operation, low insertion loss, etc. Frequency responses are key parameters to reflect the modulation efficiency of PMs at different frequencies, which require precise measurement in the fabrication and application. However, the frequency responses cannot be directly obtained by the conventional lightwave component analyzer [5], [6], since the direct photodetection of a phase-modulated signal produces no AC photocurrent.

To obtain the frequency responses of the PMs, optical spectrum analysis can be used to analyze the phase-modulated signals [7], [8]. But the poor resolution of the optical spectrum analyzer (OSA) would limit the frequency resolution of the measurement, and the responses at the low-frequency regime are unachievable. To realize high-resolution measurement, the methods based on optical interferometry [9]–[11] or two-tone modulation [12], [13] were reported. However, the former method suffers from mechanical vibrations and thermal fluctuations due to the sensitivity of the optical interferometers, while the latter requires complicated electrical spectrum analysis. To measure the vector frequency responses (i.e. the magnitude and phase responses), we have proposed an electro-optic vector analyzer (EOVA) [14] with ultrahigh resolution and broadband measurement range utilizing phase modulation to intensity modulation (PM-IM) conversion, but the frequency responses at low frequencies cannot be accurately obtained because the PM-IM converters always have a low conversion efficiency at low-frequency regime. Another problem associated with the EOVA proposed in [14] is its high wavelength dependence, making it only feasible at several specific wavelengths. In addition, all the above-mentioned approaches, a common problem is the small dynamic range because the PMs under test should work in the small signal modulation condition to ignore the errors introduced by the high-order sidebands.

In this paper, a wavelength-independent method based on stimulated Brillouin scattering (SBS) for characterizing the broadband electro-optic PMs is proposed. Benefiting from the amplification of the SBS and the high-resolution frequency sweeping, the proposed method potentially has an improved dynamic range and a sub-Hz frequency resolution. In the proposed method, a carrier-suppressed optical double-sideband (ODSB) signal with proper power and frequency is used to activate the SBS effect, by which the +1st- and −1st-order sidebands of the phase-modulated signal generated in an electro-optic PM under test are respectively amplified and attenuated. An optical single-sideband (OSSB) signal is thus achieved. Detecting the OSSB signal, the overall frequency responses can be achieved. After removing the responses of the SBS and the PD, the accurate frequency responses are obtained. An experiment based on the proposed method is performed to measure the frequency response of a commercial broadband electro-optic modulator. The frequency

Manuscript received August 9, 2018; revised December 11, 2018; accepted January 5, 2019. Date of publication January 10, 2019; date of current version February 5, 2019. This work was supported in part by the National Key R&D Program of China under Grant 2017YFF0106900, in part by the National Natural Science Foundation of China under Grant 61705103 and Grant 61527820, Jiangsu Provincial "333" Project (BRA2018042), and in part by the Fundamental Research Funds for the Central Universities under Grant NC2018005. *(Corresponding authors: Min Xue; Shilong Pan.)*

Y. Heng, M. Xue, W. Chen, and S. Pan are with the Key Laboratory of Radar Imaging and Microwave Photonics, Ministry of Education, Nanjing University of Aeronautics and Astronautics, Nanjing 210016, China (e-mail: xuemin@nuaa.edu.cn; pans@nuaa.edu.cn).

S. Han is with the 41st Research Institute of CETC, Qingdao 266000, China (e-mail: hanshunli@ei41.com).

J. Liu is with Qingdao Xingyi Electronic Equipment Co., Ltd., Qingdao 266000, China (e-mail: liujiaqing@ei41.com).

Color versions of one or more of the figures in this letter are available online at http://ieeexplore.ieee.org.

Digital Object Identifier 10.1109/LPT.2019.2891890

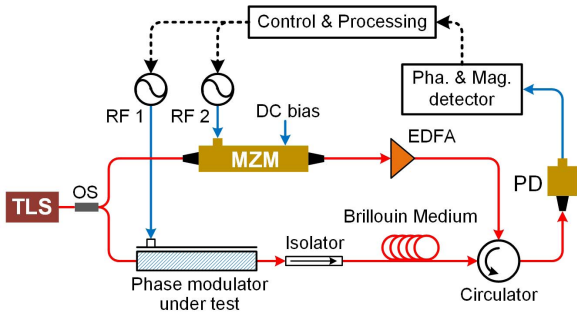

Fig. 1. The configuration of the proposed SBS-based method. TLS, tunable laser source; OS, optical splitter; MZM, Mach-Zehnder modulator; EDFA, Erbium-doped fiber amplifier; PD, photodetector; Brillouin medium, a 4.4-km single-mode fiber in the experiment.

sweeps from 10 MHz to 50 GHz and the resolution is set to 5 MHz. As compared with the method based on PM-IM conversion we previously mentioned in [14], the dynamic range is enhanced by 17.74 dB. The measurement result is verified by the conventional OSA-based method.

II. Theoretical Analysis

The schematic diagram of the proposed method based on SBS for characterizing broadband electro-optic PMs is shown in Fig. 1. An optical carrier produced from a tunable laser source is split into two portions. In the upper path, a Mach-Zehnder modulator (MZM) biased at the minimum transmission point (MITP) modulates a RF signal with an angular frequency of ω_{p} on the optical carrier. An ODSB signal with carrier suppressed is thus generated, which is used as the pump signal after proper amplification. In the lower path, a PM under test modulates a RF signal with an angular frequency of ω_{m} on the injected optical carrier. To avoid the influence of the nonlinearity, the electro-optic modulators (EOMs) work at the small signal modulation condition. Mathematically, the phase-modulated signal in the lower path can be expressed as

$$\begin{aligned} E_{\mathrm{PM}}(t) = {} & E_{\mathrm{c}} J_{+1}[\beta(\omega_{\mathrm{m}})] \exp\left[i(\omega_{\mathrm{c}}+\omega_{\mathrm{m}})t + i\frac{\pi}{2}\right] \\ & + E_{\mathrm{c}} J_0[\beta(\omega_{\mathrm{m}})] \exp(i\omega_{\mathrm{c}} t) \\ & + E_{\mathrm{c}} J_{+1}[\beta(\omega_{\mathrm{m}})] \exp\left[i(\omega_{\mathrm{c}}-\omega_{\mathrm{m}})t + i\frac{\pi}{2}\right] \end{aligned} \quad (1)$$

where E_{c} is the amplitude of the optical carrier, $\beta(\omega)$ denotes the modulation index of the PM under test at different frequencies, and $J_n(\cdot)$ represents the n-th order Bessel function of the first kind.

Let ω_{p}-$\omega_{\mathrm{m}} = \omega_{\mathrm{B}}$, where ω_{B} is the Brillouin frequency shift of the Brillouin medium. Thereby, when transmitting through the Brillouin medium, the +1st- and −1st-order sidebands are respectively amplified and attenuated by the gain and absorption of the SBS stimulated by the pump signal since the gain and absorption are located at wavelengths which are ω_{B} lower and larger than that of the pump signal, respectively [15]. The optical signal after the SBS is given by

$$\begin{aligned} E_{\mathrm{out}}(t) = {} & E_{\mathrm{c}} G(\omega_{\mathrm{m}}) J_{+1}[\beta(\omega_{\mathrm{m}})] \exp\left[i(\omega_{\mathrm{c}}+\omega_{\mathrm{m}})t + i\frac{\pi}{2}\right] \\ & + E_{\mathrm{c}} J_0[\beta(\omega_{\mathrm{m}})] \exp(i\omega_{\mathrm{c}} t) \\ & + E_{\mathrm{c}} A(\omega_{\mathrm{m}}) J_{+1}[\beta(\omega_{\mathrm{m}})] \exp\left[i(\omega_{\mathrm{c}}-\omega_{\mathrm{m}})t + i\frac{\pi}{2}\right] \end{aligned} \quad (2)$$

where $G(\omega)$ and $A(\omega)$ represent the gain and absorption of the SBS, respectively. By square-law detection, a photocurrent having an angular frequency of ω_{m} is achieved,

$$\begin{aligned} & i_{\mathrm{PM}}(\omega_{\mathrm{m}}) \\ & = \eta(\omega_{\mathrm{m}}) E_{\mathrm{c}}^2 J_{+1}[\beta(\omega_{\mathrm{m}})] J_0[\beta(\omega_{\mathrm{m}})] G(\omega_{\mathrm{m}}) \exp\left(i\frac{\pi}{2}\right) \\ & \quad + \eta(\omega_{\mathrm{m}}) E_{\mathrm{c}}^2 J_{+1}[\beta(\omega_{\mathrm{m}})] J_0[\beta(\omega_{\mathrm{m}})] A(\omega_{\mathrm{m}}) \exp\left(-i\frac{\pi}{2}\right) \end{aligned} \quad (3)$$

where $\eta(\omega)$ is the frequency response of the broadband photodetector (PD). The first term, on the right hand of the equation, is the beat note of the amplified +1st-order sideband and the optical carrier, and the second term is the component generated by the attenuated −1st-order sideband and the optical carrier. By properly adjusting the power of the pump signal, the ratio of the gain and absorption of the SBS can be very large (typ. $G(\omega)/A(\omega) > 30$ dB), so that the second term is small enough to be ignored. (3) can be simply expressed as

$$\begin{aligned} & i_{\mathrm{PM}}(\omega_{\mathrm{m}}) \\ & = \eta(\omega_{\mathrm{m}}) G(\omega_{\mathrm{m}}) E_{\mathrm{c}}^2 J_{+1}[\beta(\omega_{\mathrm{m}})] J_0[\beta(\omega_{\mathrm{m}})] \exp\left(i\frac{\pi}{2}\right) \end{aligned} \quad (4)$$

Thus, the transmission function of the PM under test is achieved, given by

$$\begin{aligned} H(\omega_{\mathrm{m}}) &= J_{+1}[\beta(\omega_{\mathrm{m}})] J_0[\beta(\omega_{\mathrm{m}})] \\ &= \frac{i_{\mathrm{PM}}(\omega_{\mathrm{m}})}{\eta(\omega_{\mathrm{m}}) G(\omega_{\mathrm{m}}) E_{\mathrm{c}}^2 \exp\left(i\frac{\pi}{2}\right)} \end{aligned} \quad (5)$$

In (5), $\eta(\omega)$ can be accurately measured by the optical heterodyne method which is a standard method recognized by National Institute of Standards and Technology (NIST) to measure the responsivity of PDs. $G(\omega)$ is the gain responses of the SBS at different frequencies, which would be slightly fluctuated with the RF frequency. To obtain the accurate frequency responses, $G(\omega)$ should be precisely characterized. To do so, a calibration process can be carried out, in which the PM is replaced by a broadband MZM biased at the quadrature transmission point (QTP). A two-step calibration process is then performed. In the first step, the intensity-modulated signal output from the MZM is directly injected into the PD. The electrical field of the produced AC photocurrent is

$$\begin{aligned} i_1(\omega_{\mathrm{m}}) = {} & 2\eta(\omega_{\mathrm{m}}) E_{\mathrm{c}}^2 J_{+1}[\beta_{\mathrm{MZM}}(\omega_{\mathrm{m}})] \\ & \times J_0[\beta_{\mathrm{MZM}}(\omega_{\mathrm{m}})] \exp\left(i\frac{\pi}{4}\right) \end{aligned} \quad (6)$$

Then, the second step is performed. The optical signal from the MZM is processed by the SBS, so the photocurrent becomes

$$\begin{aligned} i_2(\omega_{\mathrm{m}}) = {} & \eta(\omega_{\mathrm{m}}) G(\omega_{\mathrm{m}}) E_{\mathrm{c}}^2 J_{+1}[\beta_{\mathrm{MZM}}(\omega_{\mathrm{m}})] \\ & \times J_0[\beta_{\mathrm{MZM}}(\omega_{\mathrm{m}})] \exp\left(i\frac{\pi}{4}\right) \end{aligned} \quad (7)$$

From (6) and (7), $G(\omega)$ can be accurately obtained, which is

$$G(\omega_{\mathrm{m}}) = \frac{2i_2(\omega_{\mathrm{m}})}{i_1(\omega_{\mathrm{m}})} \quad (8)$$

According to (8), the transmission function of the PM under test is precisely achieved,

$$H(\omega_m) = J_{+1}[\beta(\omega_m)] J_0[\beta(\omega_m)] = \frac{i_{PM}(\omega_m) i_1(\omega_m)}{2i_2(\omega_m)\eta(\omega_m) E_c^2 \exp\left(i\frac{\pi}{2}\right)} \quad (9)$$

Benefitting from the gain of the SBS, the dynamic range is enhanced as compared with the previous methods. Since the SBS has narrow bandwidth and wide frequency tuning range, the proposed method has a broad frequency measurement range, which can be measured from several MHz to hundreds of GHz. In addition, the proposed method inherently has an ultrahigh resolution owing to the high-finesse electrical frequency sweeping. Theoretically, a sub-Hz resolution should be available.

III. Experiment and Discussion

A measurement system adopting the diagram illustrated in Fig. 1 is experimentally established. A tunable laser source (TLS, Agilent N7714A) produces an optical carrier, which is split into two paths. In the upper path, a broadband MZM (FUJITSU FTM7938EZ-A) is employed to modulate the optical carrier by the RF signal from a RF source (Agilent E8257D). To make the MZM work at MITP, a modulator bias controller (MBC, YYlabs) is employed. An erbium-doped fiber amplifier (EDFA, Amonics Inc.) is inserted to amplify the pump signal, which stimulates the SBS in a 4.4-km single mode fiber (SMF). In the lower path, a commercial broadband electro-optic PM (EOSPACE Inc.) serves as the device under test. The optical-to-electrical conversion is achieved by a calibrated broadband photodetector (Finisar, XPDV2120RA). An electrical vector network analyzer (VNA, R&S ZVA67) produces the RF signals and detects the photocurrent. In a calibration process, another broadband MZM (FUJITSU) biased at the QTP is employed. The optical spectra are monitored by an optical spectrum analyzer (OSA, Yokogawa AQ6370C).

Figure 2 shows the optical spectra of the phase-modulated signal and the SBS-processed signal when a 20-GHz RF signal with a power of 0 dBm is applied. By carefully tuning the frequency spacing between two RF signals from the RF source and the VNA, the SBS occurs in a 4.4-km SMF. In the experiment, the Brillouin frequency shift is 10.637 GHz. As can be seen, the −1st-order sideband is attenuated by 18.25 dB, while the +1st-order sideband is amplified by 17.74 dB, which brings in a 17.74-dB improvement of the dynamic range. The phase-modulated signal is converted into an OSSB signal with a sideband suppression ratio (SSR) of 36 dB, so the influence of the attenuated −1st-order sideband is ignorable. It is worth to mention that the Rayleigh backscattering is also activated by the pump signal, as shown in Fig. 2, but it has no influence on the measurement results since the power is much lower than the useful optical components (e.g., the optical carrier and the amplified +1st-order sideband) and is incoherent with the SBS-processed signal.

Figure 3 shows the magnitude responses measured with and without the SBS and the gain of the SBS at different frequencies obtained in the calibration process. In this case,

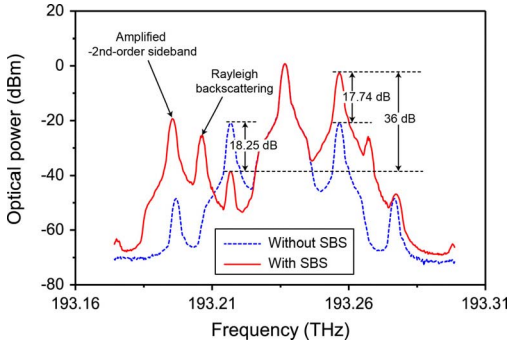

Fig. 2. Optical spectra of the phase-modulated signal from the PM under test with and without the SBS.

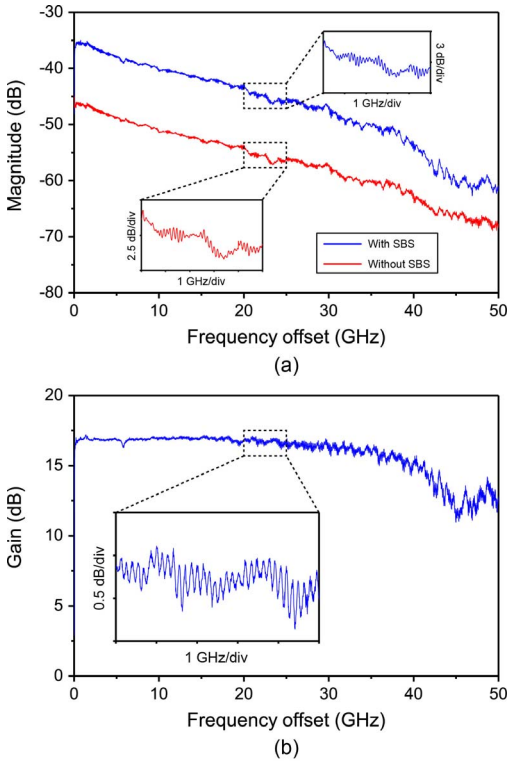

Fig. 3. (a) The magnitude responses measured with and without the SBS and (b) the obtained response of the SBS gain.

a broadband MZM biased at the QTP is serviced as the modulator under test. There are 9999 measurement points from 10 MHz to 50 GHz, which leads to a resolution of 5 MHz. Benefitting from the high resolution, the magnitude responses of the MZM-based link with and without the SBS are precisely measured, as shown in Fig. 3(a), wherein the ripples are finely characterized, as shown in the insets of Fig. 3(a). According to the two measured responses, the gain of the SBS at different frequencies is precisely calculated by (8), as illustrated in Fig. 3(b). The measured gain is about 17.5 dB, which agrees with the gain obtained in Fig. 2. The ripples in the achieved gain response are finely observed, as shown the inset of Fig. 3(b). It should be noted that the gain decreases at the high frequencies, because the working bandwidth of the MZM used to generate the pump signal is limited, which leads to the small gain at the high-frequency regime.

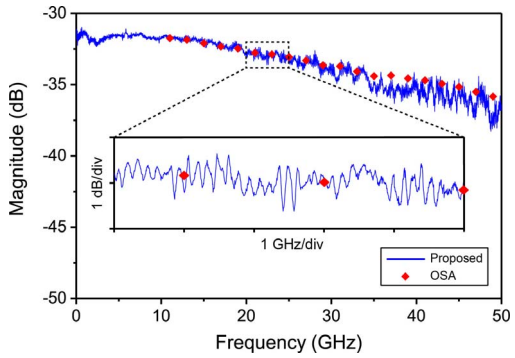

Fig. 4. The frequency responses measured by the proposed SBS-based method and the conventional OSA-based method.

Figure 4 shows the frequency responses obtained by the proposed SBS-based method and the conventional OSA-based method. By removing the response of the calibrated PD and the SBS gain from the observed overall frequency responses, the frequency response of the PM (blue solid line) is accurately achieved. The measurement resolution is 5 MHz. Thanks to the high resolution, the internal fine structures are clearly obtained, as shown in the inset of Fig. 4. The resolution can be further improved by employing a laser source with ultra-narrow linewidth and increasing the measurement points. To achieve the theoretical sub-Hz resolution, a laser source with a linewidth of sub-Hz is required and the measurement points should be large enough to ensure that the frequency spacing between the neighboring points reaches sub-Hz level. For instance, to achieve 100-mHz resolution in a frequency range of 10 kHz, 100001 measurement points are required. The response characterized by the conventional OSA-based method (red solid diamonds) is also plotted in Fig. 4, by which the frequency response measured by the proposed method is verified.

It should be noted that the phase response of the PM is theoretically measurable, but the phase response is unachievable in the experiment because the delay introduced by the 4.4-km SMF (to stimulate the SBS) is sensitive to the temperature variation. To achieve the phase response measurement, a complex setup is required to carefully control the temperature and isolate the vibration. Alternatively, an As_2S_3 waveguide [16] with careful temperature control and vibration isolation can be employed to generate the SBS, by which the phase response would be measurable. In addition, the multi-stage SBS amplification [17] can be employed to improve the performance of the proposed method, as it has evident superiority in terms of high selectivity and low noise in the high gain conditions.

IV. Conclusion

In conclusion, a method based on SBS for characterizing the frequency responses of broadband electro-optic PMs is proposed and experimentally demonstrated, which features ultrahigh frequency resolution, large dynamic range, and broadband measurement range. In the experiment, the frequency response of a commercial broadband PM is measured in the frequency range from 10 MHz to 50 GHz with a resolution of 5 MHz, which is verified by the conventional OSA-based method.

References

[1] D. Ly-Gagnon, S. Tsukamoto, K. Katoh, and K. Kikuchi, "Coherent detection of optical quadrature phase-shift keying signals with carrier phase estimation," *J. Lightw. Technol.*, vol. 24, no. 1, pp. 12–21, Jan. 2006.

[2] J. Yao, "Microwave photonics," *J. Lightw. Technol.*, vol. 27, no. 3, pp. 314–335, Feb. 1, 2009.

[3] S. L. Pan and J. Yao, "Photonics-based broadband microwave measurement," *J. Lightw. Technol.*, vol. 35, no. 16, pp. 3498–3513, Aug. 15, 2017.

[4] M. Xue, S. Liu, and S. Pan, "High-resolution optical vector analysis based on symmetric double-sideband modulation," *IEEE Photon. Technol. Lett.*, vol. 30, no. 5, pp. 491–494, Mar. 1, 2018.

[5] P. D. Hale and D. F. Williams, "Calibrated measurement of optoelectronic frequency response," *IEEE Trans. Microw. Theory Techn.*, vol. 51, no. 4, pp. 1422–1429, Apr. 2003.

[6] "High-speed lightwave component analysis," Agilent Technol., Palo Alto, CA, USA, Appl. Note 1550-6, 2000.

[7] R. Tench, J.-M. Delavaux, L. Tzeng, R. Smith, L. Buhl, and R. Alferness, "Performance evaluation of waveguide phase modulators for coherent systems at 1.3 and 1.5 μm," *J. Lightw. Technol.*, vol. 5, no. 4, pp. 492–501, Apr. 1987.

[8] Y. Shi, L. Yan, and A. E. Willner, "High-speed electrooptic modulator characterization using optical spectrum analysis," *J. Lightw. Technol.*, vol. 21, no. 10, pp. 2358–2367, Oct. 2003.

[9] E. H. W. Chan and R. A. Minasian, "A new optical phase modulator dynamic response measurement technique," *J. Lightw. Technol.*, vol. 26, no. 16, pp. 2882–2888, Aug. 15, 2008.

[10] F. P. Romstad, D. Birkedal, J. Mork, and J. A. Hvam, "Heterodyne technique for measuring the amplitude and phase transfer functions of an optical modulator," *IEEE Photon. Technol. Lett.*, vol. 14, no. 5, pp. 621–623, May 2002.

[11] N. Caponio, P. Gambini, and M. Puleo, "Characterization of the dynamic response of a waveguide phase modulator by means of an optical frequency discriminator," Nat. Inst. Standards Technol., Gaithersburg, MD, USA, NIST Special Pub. 792, 1990, pp. 79–82.

[12] S. J. Zhang, H. Wang, X. H. Zou, Y. L. Zhang, R. G. Lu, and Y. Liu, "Self-calibrating measurement of high-speed electro-optic phase modulators based on two-tone modulation," *Opt. Lett.*, vol. 39, no. 12, pp. 3504–3507, Jun. 2014.

[13] S. Zhang, C. Zhang, H. Wang, X. Zou, Y. Liu, and J. E. Bowers, "Calibration-free measurement of high-speed Mach–Zehnder modulator based on low-frequency detection," *Opt. Lett.*, vol. 41, no. 3, pp. 460–463, 2016.

[14] M. Xue, Y. Heng, and S. Pan, "Ultrahigh-resolution electro-optic vector analysis for characterization of high-speed electro-optic phase modulators," *J. Lightw. Technol.*, vol. 36, no. 9, pp. 1644–1649, May 1, 2018.

[15] W. Li, N. H. Zhu, L. X. Wang, and H. Wang, "Broadband phase-to-intensity modulation conversion for microwave photonics processing using Brillouin-assisted carrier phase shift," *J. Lightw. Technol.*, vol. 29, no. 24, pp. 3616–3621, Dec. 15, 2011.

[16] R. Pant *et al.*, "On-chip stimulated Brillouin scattering," *Opt. Express*, vol. 19, no. 9, pp. 8285–8290, Apr. 2011.

[17] W. Wei, L. Yi, Y. Jaouën, M. Morvan, and W. Hu, "Brillouin rectangular optical filter with improved selectivity and noise performance," *IEEE Photon. Technol. Lett.*, vol. 27, no. 15, pp. 1593–1596, Aug. 1, 2015.